Clinical Oncology 36 (2024) 562–575

Contents lists available at ScienceDirect

Clinical Oncology

journal homepage: www.clinicaloncologyonline.net

Overview

Paediatric Anatomical Models in Radiotherapy Applications

V. Apte [*], A. Ghose [†‡§¶||], C.A. Linares [**], S. Adeleke [**††], V. Papadopoulos [‡‡], E. Rassy [§§], S. Boussios [†††¶¶|||||***]

[*] Medical School, University College London, London WC1E 6BT, UK
[†] Department of Medical Oncology, Medway NHS Foundation Trust, Gillingham ME7 5NY, UK
[‡] Department of Medical Oncology, Barts Cancer Centre, St Bartholomew's Hospital, Barts Heath NHS Trust, London EC1A 7BE, UK
[§] Department of Medical Oncology, Mount Vernon Cancer Centre, East and North Hertfordshire Trust, London HA6 2RN, UK
[¶] Health Systems and Treatment Optimisation Network, European Cancer Organisation, Brussels 1040, Belgium
[||] Oncology Council, Royal Society of Medicine, London W1G 0AE, UK
[**] Guy's Cancer Centre, Guy's and St Thomas' NHS Foundation Trust, London SE1 9RT, UK
[††] School of Cancer & Pharmaceutical Sciences, King's College London, Strand, London WC2R 2LS, UK
[‡‡] Department of Urology, Kent and Canterbury Hospital, Canterbury CT1 3NG, UK
[§§] Department of Medical Oncology, Gustave Roussy Institut, Villejuif 94805, France
[¶¶] Kent Medway Medical School, University of Kent, Canterbury CT2 7LX, UK
[|||||] Canterbury Christ Church University, Canterbury CT2 7PB, UK
[***] AELIA Organization, 9th Km Thessaloniki – Thermi, Thessaloniki 57001, Greece

Abstract

Anatomical models have key applications in radiotherapy, notably to help understand the relationship between radiation dose and risk of developing side effects. This review analyses whether age-specific computational phantoms, developed from healthy subjects and paediatric cancer patient data, are adequate to model a paediatric population. The phantoms used in the study were International Commission on Radiological Protection (ICRP), 4D extended cardiac torso (XCAT) and Radiotherapy Paediatric Atlas (RT-PAL), which were also compared to literature data. Organ volume data for 19 organs was collected for all phantoms and literature. ICRP was treated as the reference for comparison, and percentage difference (P.D) for the other phantoms were calculated relative to ICRP. Overall comparisons were made for each age category (1, 5, 10, 15) and each organ. Statistical analysis was performed using Microsoft Excel (version 16.59). The smallest P.D to ICRP was for Literature (-17.4%), closely followed by XCAT (26.6%). The largest was for RT-PAL (88.1%). The rectum had the largest average P.D (1,049.2%) and the large bowel had the smallest (2.0%). The P.D was 122.6% at age 1 but this decreased to 43.5% by age 15. Linear regression analysis showed a correlation between organ volume and age to be the strongest for ICRP ($R^2 = 0.943$) and weakest for XCAT ($R^2 = 0.676$). The phantoms are similar enough to ICRP for potential use in modelling paediatric populations. ICRP and XCAT could be used to model a healthy population, whereas RT-PAL could be used for a population undergoing/after radiotherapy.

Key words: Age-specific; Organ volume; Paediatric cancer; Phantoms; Radiotherapy

Introduction

Radiotherapy uses ionising radiation to kill cancer cells. As the radiation beams damage normal tissue around the tumour as well as cancerous tissue, patients are at risk of developing many side effects, both early and late [1]. One very rare, but serious complication of radiotherapy in children or the paediatric population is the risk of developing second malignancies [2]. The probability of developing the aforesaid is influenced by several factors including radiation dose, volume of tissue irradiated, and age of treatment commencement, to name a few [3].

Due to the plethora of side effects, anatomical models have key applications in paediatric radiotherapy. They could potentially be used as a tool to reconstruct doses for historical cohorts (when there was no imaging data) so that

Author for correspondence: S. Boussios, Health, and Social Care, Canterbury Christ Church University, Canterbury, UK.
E-mail address: stergiosboussios@gmail.com (S. Boussios).

https://doi.org/10.1016/j.clon.2024.06.051

epidemiology studies can be conducted. They can be used as a quality assurance tool in clinical settings, to optimise radiotherapy protocols. And finally, they can be used to estimate the dose to organs that are not imaged in clinical settings, as typically only the treated region is imaged. Knowing the dose delivered to all of the body is important to understand the relationship between dose and side-effects, and to mitigate the latter – this would in turn help improve radiotherapy outcomes. The models, also known as phantoms, attempt to provide an accurate representation of human anatomy. They reflect the differences in growth and development, and therefore organ size, between the ages 0 to 16, according to which the radiation dosage can be calculated. Organ size is very important when deciding dosage because radiation absorption directly depends on size, which is known as the dose-volume effect – there is a relationship between the volume of the organ irradiated and the degree of organ toxicity faced by the patient, which is why it is important to amend dosage according to organ volume [4,5]. Even though there are newborn reference phantoms, newborns are rarely treated with radiotherapy because radiation would cause serious organ damage so this review will exclude newborn phantoms. The comparative focus is on organ volume and this will demonstrate the impact that disease and radiotherapy can have on organ characteristics, and then in turn will highlight the relevance of various anatomical models for modelling a cancer population. There are 19 organs of interest because these are especially related to the late side effects seen in children.

The International Commission on Radiological Protection (ICRP) Publication 143 provides a deep insight into the ICRP paediatric reference phantoms, including how they were developed [6]. The ICRP phantoms are a series of 10 models for the following ages, both male and female: newborn, 1, 5, 10 and 15 years. The construction of these phantoms follows a set of steps with the first being the selection and segmentation of computed tomography (CT) data on organs and tissues to form a traditional voxel phantom. The internal organs are then modelled to the reference organ volume via the addition or removal of individual layers of voxels. The final step in the development of these phantoms was to further modify the voxel phantoms so that they comply with the phantom structure in Publication 110. Publication 110 describes the development of the adult male and female reference phantoms and it provides a database which can be used when calculating radiation dosage [7].

4D extended cardiac torso (XCAT) paediatric phantoms were developed by Norris *et al.* for the following ages, both male and female: newborn, 1, 5, 10 and 15 years [8]. They are as detailed as the adult XCAT phantoms produced by the same authors. Each of the paediatric phantoms were created using CT datasets of healthy patients from the Duke University database. The reference values from ICRP Publication 89 for height and weight for each of these ages and for both genders were used when selecting the appropriate datasets for each phantom. The CT data covered the thorax, abdomen and part of the head. Major organs and structures were separated from this data and were used to form an initial model. The rest of the body was manually completed by using scaled versions of the adult XCAT phantoms created by the same authors as well as other models based on cadaver data – this formed the top of the head, arms and legs in the phantom. ICRP Publication 89 also gives reference values for organ mass and these were matched to the organ masses in each phantom [8]. The follow-on work led to the development of models for more ages than the ones listed above [9].

The in-house synthetic models (RT-PAL) developed by Veiga *et al.* are created differently [10]. Whilst the other two are based off healthy paediatric patient data, these models have been developed using CT imaging data from historical paediatric cancer patients that have had radiotherapy, namely craniospinal irradiation (CSI). Whilst the other phantoms merge data from different sources to obtain values for mass and volume, the RT-PAL phantom does not do this. The reference model is formed via three main steps. Step 1: pre-processing cancer patient data to generate a template that could be used for spatial normalisation. Step 2: groupwise image registration, which is an iterative process of registering all the CT images/data together to form an average image model, and then updating this reference image with the produced average model. Image registration overlays images taken at different times and/or angles to then align the images [11]. Step 3: atlas construction to generate a template CT and contours. This approach enables the standardisation of a heterogenous population in an objective way, whilst averaging the information on anatomy, including mass and volume. This reference model was constructed with the motivation of enabling voxel-based analysis of radiation-induced side effects, but also has relevance as phantoms for radiotherapy applications [10]. The reference model was a starting point and since then age-specific models for both genders have been developed (RT-PAL) – this review will look at these age-specific models [12].

Comparison of literature data to the phantoms will also be conducted. ICRP Publication 89 and ICRP Publication 23 provide a strong base as they both have information for almost all organs, but since this review is also looking at the ICRP phantoms, the attempt is to find literature outside of these publications for a meaningful comparison [13,14]. Literature can contain normal human anatomy research, including studies that may look at how the human body and its organs change across different stages in life. These studies are mainly conducted using imaging modalities but can also use cadaver data and can be for, but are not limited to, different diseases, ages and genders – the outcome of these studies could be organ volume, mass or even length. Literature data will be obtained through papers/studies that can be accessed via library databases and will be compared to the phantoms in order to see what other factors could potentially affect organ volume.

Aims and Objectives

This review aims to compare the phantoms' builds by investigating the differences in organ volume and seeing how they compare to each other and to literature data. This will help inform the need for specific phantoms for paediatric radiotherapy, where there may be anatomical differences between healthy and cancer patients. To achieve this aim, it is essential to make comparisons between a reference phantom and the other phantoms and literature. For the purpose of this review, the ICRP phantom will be treated as the reference model (XCAT is the commercial model and RT-PAL is the in-house model) and any comparisons will be made to this phantom. ICRP was chosen as the reference for one main reason - the ICRP is a registered charity that provides authoritative sources of guidance on protection against ionising radiation through its publications; it is the main governing body and is responsible for setting policy and giving direction, essentially making ICRP the gold standard phantom.

Methods

The phantoms used in this review are the ICRP, XCAT and RT-PAL (Figure 1) – at present these are closed-source and only accessible in-house. These are the organs of interest: bladder, brain, eyes, gallbladder, heart, kidneys, large bowel, liver, lungs, oesophagus, oral cavity, pancreas, rectum, salivary glands, small bowel, spinal cord, spleen, stomach and thyroid gland. All the data was collected together and processed on Microsoft Excel (version 16.59).

Phantom Data

The data was organised into a cohesive format for analysis, as shown in Figures 2 and 3. Data for organ volume only was gathered.

ICRP

There were 8 ICRP models in total (4 male, 4 female), with a mean age of 7.8 years (range: 1–15 years). There were spreadsheets for each age (1, 5, 10 and 15 years old) and both genders. As computational phantoms are genderless until the age of 15, there was no difference in value for organ volume between genders for ages 1, 5, and 10 but for age 15, a mean value was calculated as the focus is on age and organs rather than gender.

There were 75 XCAT models in total (37 male, 38 female), with a mean age of 9.2 years (range: 1–18 years). For the organ sheets, the age and organ volume columns were pasted onto the respective sheets under the correct headings in Figure 3. For the age sheets, for each organ, averages had to be calculated to obtain 4 separate values. This was done so that key ages can be compared across multiple phantoms – the reference ICRP phantoms are for ages 1, 5, 10 and 15, so the XCAT values must be for the same ages to allow for a fair comparison. The following age brackets were used to group the data together: 1–5 for the 1-year-old value, 5–10 for the 5-year-old value, 10–15 for the 10-year-old value and 15 and above for the 15-year-old value. A respective standard deviation (S.D) also had to be calculated.

There were 74 RT-PAL models in total (39 male, 35 female), with a mean age of 7.61 years (range: 3–14 years). For the organ sheets, the process was the same as the XCAT data. For the age sheets, again an average and S.D were calculated. The age brackets used were smaller because RT-PAL has a narrower age range and a lower mean age. They were as follows – 1–4 for the 1-year-old value, 4–7 for the 5-year-old value, 7–11 for the 10-year-old value and 11–15 for the 15-year-old value.

PubMed and Google Scholar were used when searching for papers on organ volume and mass. Firstly, the search was for papers that specifically looked at paediatric (or adult) organ volume. The studies did not necessarily have to

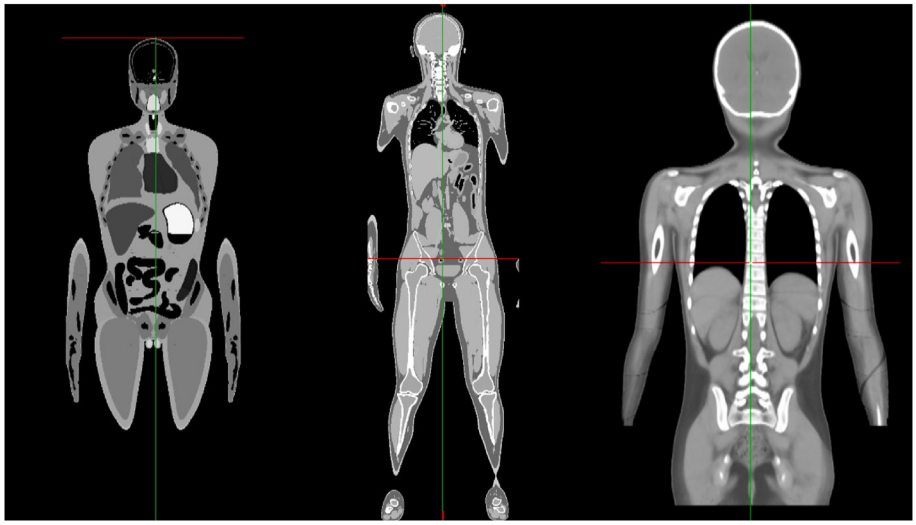

Fig 1. Images of the three phantoms to highlight how they visually look different. Left: ICRP. Centre: XCAT. Right: RT-PAL.

	Phantoms and respective organ volumes (ml)				Standard Deviation	
Organ	ICRP	XCAT	Literature	RT-PAL	XCAT	RT-PAL
Bladder						
Brain						
Eyes						
Gallbladder						
Heart						
Kidneys						
Large Bowel						
Liver						
Lungs						
Oesophagus						
Oral Cavity						
Pancreas						
Rectum						
Salivary Glands						
Small Bowel						
Spinal Cord						
Spleen						
Stomach						
Thyroid						

Fig 2. An image of a blank Table to show how the phantom data was organised on each age sheet (for the ages 1, 5, 10 and 15).

be for healthy subjects and could contain data from cadavers or for patients with different diseases – the goal was to find reported data on organ volume across developmental stages. After many searches, it was difficult to find organ volume studies for all the organs in question, so the search was expanded to organ mass. Finding data for organ mass would also be suitable as these values could be converted to volume using the density values found in ICRP Publication 143 (example shown in Figure 4) and using Eq. 1.

$$Volume = \frac{Mass}{Density} \quad \text{Eq. 1}$$

Some literature contained formulae to calculate organ volume according to age, weight, and height, for which the height and weight of the ICRP reference models found in ICRP Publication 143 were used. The values are the same for both genders for ages 1, 5 and 10 but for age 15, the mean height and weight of the two genders had to be calculated (Figure 5).

Sourcing at least one paper for each organ proved to be difficult due to the greater relative availability of papers regarding volume/mass for some organs than others. As mentioned previously, Publication 89 and Publication 23 provided a good foundation for the literature search and the citations in these publications were used to find the original papers from which they were based on. Because of a lack of literature related to organs such as the oesophagus, salivary glands, small and large bowels etc., the masses in the ICRP Publications were used and converted to volumes using Eq. 1. Excluding the ICRP Publications, a total of 16 studies have been included in this review (Table 1).

Data Analysis

A bar chart was created on each of the age sheets to see if the models were similar to the ICRP reference model at certain ages. On each of the organ sheets, a scatter graph was plotted with all 4 datasets. Each respective regression line equation was used to get values for each age from 1 to 15 for each phantom (Figure 6). A percentage difference (P.D) with respect to the ICRP phantom for each of the other three phantoms was calculated using Eq. 2. A mean P.D and S.D for each age was calculated, as well as an overall mean P.D and S.D across all ages, so that there would be a single overall P.D and S.D value for each organ.

$$percentagedifference = \frac{(XCAT \vee Literature \vee RTPALvalue - ICRPvalue)}{ICRPvalue} x100 \quad \text{Eq. 2}$$

Results

The purpose of this review is to compare the phantoms and literature to the reference ICRP phantom and the findings below help address the main research question. The oral cavity has been excluded from the analysis because of a lack of ICRP data for that organ so there is nothing to compare it to.

Age	RT-PAL Volume	ICRP Volume	XCAT Volume	Literature Volume

Fig 3. An image of the headings of the Table on the organ sheets to show how the data was organised here.

$$Equation 1: Volume = \frac{Mass}{Density}$$

	Medium	H_1	C_6	N_7	O_8	Na_{11}	Mg_{12}	P_{15}	S_{16}	Cl_{17}	K_{19}	Ca_{20}	Fe_{26}	I_{53}	Density (g/cm^3)
40	Thyroid	10.4	11.8	2.5	74.5	0.2	0.0	0.1	0.1	0.2	0.0	0.1	0.0	0.1	1.05
41	Urinary bladder wall	10.5	9.6	2.6	76.1	0.2	0.0	0.2	0.2	0.3	0.0	0.3	0.0	0.0	1.04
42	Ovaries	10.5	24.8	2.7	61	0.1	0.0	0.2	0.3	0.2	0.0	0.2	0.0	0.0	1.05
43	Adrenal glands	10.5	23.3	2.8	62.5	0.1	0.0	0.2	0.3	0.2	0.0	0.2	0.0	0.0	1.03
44	Oesophagus wall	10.4	22.7	2.8	63	0.1	0.0	0.2	0.3	0.2	0.0	0.2	0.0	0.0	1.03
45	Generic soft tissue (several organs)	10.5	24.6	2.7	61.2	0.1	0.0	0.2	0.3	0.2	0.0	0.2	0.0	0.0	1.03

Fig 4. An image of a section of the Table in Publication 143 that lists the densities for organs in the 1-year-old male phantom. There are Tables like this for each of the ICRP phantoms, from newborn to 15 years old for both genders (10 in total). The densities were generally the same for both genders but differed across the ages.

Age

Figures 7–10 show that organ volumes for the gallbladder, rectum and thyroid seem very different across the phantoms, whereas the brain, liver and salivary glands volumes seem very similar. To obtain comparable values, on each of the age sheets, for each organ, P.Ds relative to ICRP for each phantom and literature were calculated using Eq. 2. Following that, using the 'AVERAGE' and 'STDEV.S' functions, an average of the three P.Ds and S.D for each organ was obtained, as well as an overall average mean and S.D values across the organs, for each age category – the latter is the 'AVERAGE' row in Table 2.

Table 2 consists of the results of these calculations. The 'AVERAGE' row shows that as age increases the mean P.D decreases. Initially, it is very high at 122.6% for age 1 and it decreases down to 43.5% for age 15. The S.D tends to fall as age increases, implying that there is a relatively smaller spread of P.D data as age increases. This demonstrates an inverse relationship between age and mean P.D in organ volume, therefore meaning that as age increases, the phantoms overall are more like the ICRP. Some organs, such as the heart, lungs, kidneys etc., initially have a positive P.D at age 1 but by age 15, the P.D is negative, meaning that the average organ volume for the other phantoms is higher than the ICRP at first but as age increases, the average falls to be below the ICRP.

Organ

Table 3 condenses the important values from Figure 6 for each organ. The 'overall mean % difference' column is a mean of the prior 3 columns and the S.D is for this mean. The findings in Table 3 show that the mean P.D to the ICRP phantom is highest for the rectum (1,049.2%) and the lowest is for the large bowel (2.0%). The XCAT brain P.D is particularly low (-0.9%) and the RT-PAL rectum P.D is particularly high (1,620.8%). The rectum has the highest S.D (808.3%) and the liver has the lowest (2.3%). Other than the rectum, the following organs: gallbladder, spleen, bladder, stomach and thyroid, also have fairly large mean P.Ds. An extra 'AVERAGE' row has been added to see if one phantom is more similar to the ICRP than the others, across all of the organs. The S.D of 53.0% is for the mean value to the left of it (32.4%), just like the rest of the S.D column. The average Literature P.D is the lowest of the three (-17.4%) and the average RT-PAL P.D is the highest (88.1%), meaning that across the organs, the literature data is the most similar to ICRP and RT-PAL is the least similar. Excluding the outlier rectum P.D, the average P.Ds for XCAT and RT-PAL are 0.0% and -2.1% respectively.

Correlation

Table 4 lists all the linear regression equations and Supplementary Figures 1-19 show the linear fits for all organs.

The 'AVERAGE' row in Table 5 shows that overall, the ICRP linear fits are the best (highest average R^2 value of 0.943) and the XCAT ones are the worst (lowest average R^2 value of 0.676). The linear fits are also very good for the literature models (0.915). All of the p-values for the RT-PAL and XCAT models are <0.05 i.e., they are all statistically significant. However, a few of the ICRP and literature

	Height (cm)		Mass (kg)		Surface area (m^2)	
Age	Male	Female	Male	Female	Male	Female
Newborn	51	51	3.5	3.5	0.24	0.24
1 year	76	76	10	10	0.48	0.48
5 years	109	109	19	19	0.78	0.78
10 years	138	138	32	32	1.12	1.12
15 years	167	161	56	53	1.62	1.55
Adult	176	163	73	60	1.90	1.66

Fig 5. An image of the Table in Publication 143 that contains the height and weight (mass) information.

Table 1
All the organs and the citations of the relevant literature – no data was found for the rectum and spinal cord, so they have been left blank

Organ	Name of Paper(s)	Citation	Type of data
Bladder	• 'ICRP Publication 89'	[13]	• Organ mass
Brain	• 'Changes in brain weights during the span of human life: relation of brain weights to body heights and body weights'	[15]	• Raw data on organ masses
Eyes	• 'ICRP Publication 89'	[13]	• Organ mass
Gall bladder	• 'ICRP Publication 89'	[13]	• Organ mass
	• 'ICRP Publication 23'	[14]	• Raw data on organ volume
	• 'Association of Gallbladder Volume and Wall Thickness With Acute Appendicitis in Pediatric Patients'	[16]	
Heart	• 'Body Length and Organ Weights of Infants and Children'	[17]	• Raw data on organ masses
		[18]	• Raw data on organ masses
	• 'Normal Organ Weights in Women: Part I-The Heart'	[19]	
	• 'Normal Organ Weights in Men: Part I-The Heart'		
Kidneys	• 'Advanced Kidney Volume Measurement Method Using Ultrasonography with Artificial Intelligence-Based Hybrid Learning in Children'	[20]	• Formula to calculate volume
Large Bowel	• 'ICRP Publication 89'	[13]	• Organ mass
Liver	• 'A formula to calculate the standard liver volume in children and its application in pediatric liver transplantation'	[21]	• Formula to calculate volume
Lungs	• 'Body Length and Organ Weights of Infants and Children'	[17]	• Raw data on organ masses
		[22]	• Raw data on organ masses
	• 'Normal Organ Weights in Women: Part II-The Brain, Lungs, Liver, Spleen, and Kidneys'	[23]	
	• 'Normal Organ Weights in Men: Part II-The Brain, Lungs, Liver, Spleen, and Kidneys'		
Oesophagus	• 'ICRP Publication 89'	[13]	• Organ mass
Oral Cavity	• 'Evaluation of tongue volume and oral cavity capacity using cone-beam computed tomography'	[24]	• Raw data on organ volume
Pancreas	• 'Organ weight in 684 adult autopsies: new Tables for a Caucasoid population'	[25]	• Organ mass
	• 'ICRP Publication 89'	[13]	• Organ mass
Rectum			
Salivary Glands	• 'ICRP Publication 89'	[13]	• Organ mass
Small Bowel	• 'ICRP Publication 89'	[13]	• Organ mass
Spinal Cord			
Spleen	• 'Normal values of Spleen Length and Volume: An Ultrasonographic Study in Children'	[26]	• Raw data on organ length and volume
Stomach	• 'SOME GRAPHS AND TABLES ILLUSTRATING THE GROWTH OF THE HUMAN STOMACH'	[27]	• Organ mass
	• 'ICRP Publication 89'	[13]	• Organ mass
Thyroid	• 'The determination of thyroid volume by ultrasound and its relationship to body weight, age, and sex in normal subjects'	[28]	• Formula to calculate volume

models (4 and 3 respectively) are >0.05 so they are statistically non-significant. The R^2 values for the brain (RT-PAL) and gallbladder (XCAT) are the lowest on the table (0.170 and 0.177 respectively), again with p-values <0.05, suggesting that their regression lines are not the best models for their data and this is statistically significant.

Discussion

We aim to compare different paediatric phantoms to see which phantoms could potentially be used to model a paediatric population. A major reason for the differences could be due to inter-patient variability; nevertheless, this review looks to investigate any other causes.

Organ and Correlation

Table 3 is based on the values obtained using the linear regression equations and Table 5 contains the R^2 and p-values for the same regression models, so these results can be interpreted simultaneously. The ICRP average R^2 value is the highest of the four (0.943), meaning that those fits are

	Phantom				Relative % difference to ICRP			Mean %	S.D of %
Age	ICRP	XCAT	Literature	RT-PAL	XCAT	Literature	RT-PAL	difference	difference
1									
2									
3									
4									
5									
6									
7									
8									
9									
10									
11									
12									
13									
14									
15									
			Overall mean % difference and S.D:						

Fig 6. An image of a blank Table.

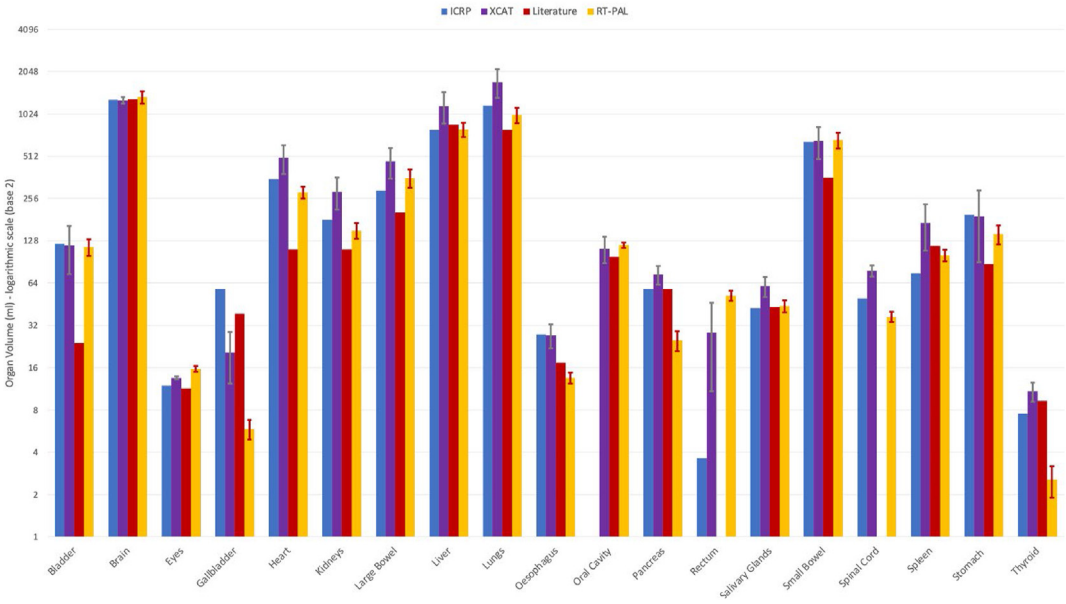

Fig 7. 1 year old. Bars represent the standard deviation.

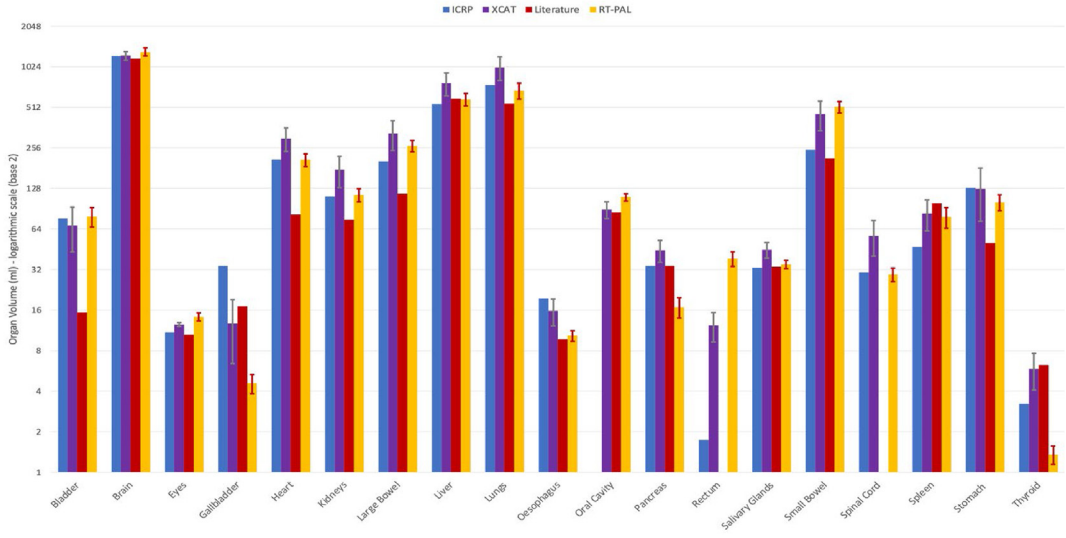

Fig 8. 5 years old. Bars represent the standard deviation.

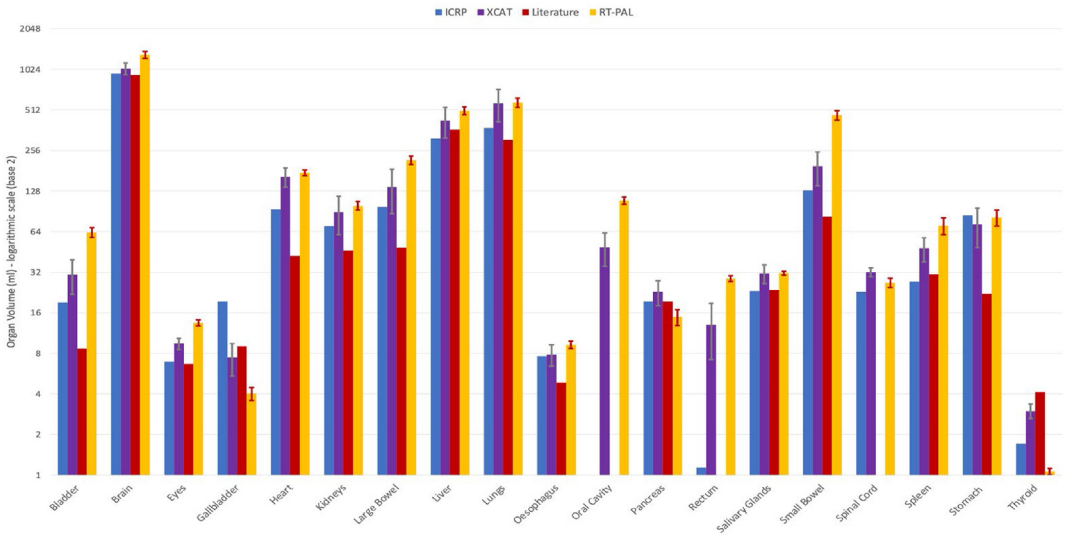

Fig 9. 10 years old. Bars represent the standard deviation.

very good overall so any comparisons to the ICRP regression models are likely to be reasonable.

Of the three, literature data is the most similar to ICRP because volumes on average are only 17.4% smaller. Of all the literature P.Ds, the smallest are for the following organs: brain, eyes, pancreas and salivary glands (all within -5 to 5%). However, for all of these except the brain, the data from Publication 89 was used as the literature value. This publication is also used in the formation of the ICRP phantoms, meaning that volume values for the literature and ICRP would be very similar, hence the low P.D to ICRP. The literature paper on the brain looked at over 20,000 autopsy reports, and only healthy brains, without pathological lesions, were weighed and studied [15]. The low P.D to ICRP can show that there is not much change in brain mass after an individual passes away, and this is true across all ages. The R^2 values for the ICRP and literature fit for all 4 of these organs indicate that the regression models are good/very good fits for the respective data. But the p-values for the brain and eyes (both ICRP and literature) are >0.05, which implies that even though those models are a good fit, they are not statistically significant, so the P.D calculated may not necessarily be valid.

However, for some organs such as the bladder and stomach, even though the values from Publication 89 have been used, the P.Ds to ICRP are relatively quite high (within the range -60 to -80%). (The negative value indicates that the ICRP value is larger than the literature.) The p-values for both organs (ICRP and literature) are <0.05 so the fits are statistically significant as well. Since the ICRP phantoms are based on CT/Magnetic Resonance Imaging (MRI) scans of real people, it is possible that the bladders and stomachs of

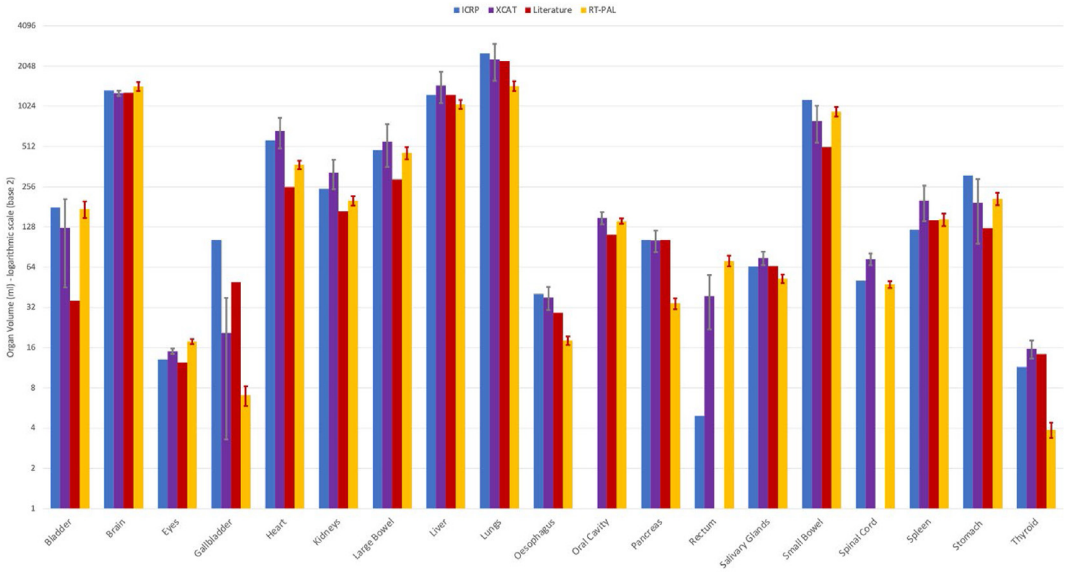

Fig 10. 15 years old. Bars represent the standard deviation.

Table 2
Overall mean percentage difference relative to ICRP and standard deviation values for each age category and the corresponding organ. ICRP is being compared to everything averaged together. A negative value for percentage difference means that the ICRP value is larger than the other phantom value and vice versa

Organ	1 year old		5 years old		10 years old		15 years old	
	Mean % difference	S.D	Mean % difference	S.D	Mean % difference	S.D	Mean % difference	S.D
Bladder	78.8	143.5	-29.1	44.5	-29.2	44.2	-37.3	39.2
Brain	14.9	20.9	1.5	5.7	1.5	2.8	-0.7	6.6
Eyes	41.7	48.9	13.3	17.4	13.5	18.1	15.2	20.7
Gallbladder	-64.8	13.2	-66.2	18.7	-62.6	28.3	-74.9	21.2
Heart	35.6	78.5	-5.7	52.6	-15.6	55.0	-24.1	37.3
Kidneys	11.0	39.8	9.6	45.7	0.9	50.5	-6.0	34.0
Large Bowel	37.2	86.2	16.1	52.9	17.8	45.5	-9.5	27.9
Liver	37.4	22.2	19.9	19.4	19.2	25.3	1.5	16.5
Lungs	29.7	41.2	-0.4	31.9	-0.1	41.8	-22.0	18.4
Oesophagus	-3.9	29.5	-38.6	17.1	-29.7	25.6	-29.7	24.7
Oral Cavity								
Pancreas	-1.8	20.8	-6.5	40.9	-9.9	42.4	-22.7	38.0
Rectum	1,735.3	973.8	1,359.7	1,061.1	1,002.4	452.8	1,020.3	464.3
Salivary Glands	23.7	19.5	14.3	18.7	15.8	23.5	-1.1	17.1
Small Bowel	92.5	153.3	59.1	64.2	-13.3	26.9	-34.7	19.2
Spinal Cord	28.3	16.1	42.0	63.8	15.6	58.4	19.6	36.5
Spleen	82.7	73.3	84.4	22.6	72.5	48.6	33.8	26.8
Stomach	-30.6	38.0	-28.1	30.2	-28.5	26.4	-43.3	14.4
Thyroid	59.4	90.7	39.0	84.3	0.6	58.7	-1.0	56.6
AVERAGE	**122.6**	**404.3**	**82.5**	**320.8**	**53.9**	**238.4**	**43.5**	**245.1**

Table 3
Overall percentage differences relative to ICRP and their respective standard deviations for each organ. The literature values for the rectum and spinal cord have been left blank due to a lack of data. A negative value for percentage difference means that the ICRP value is larger than the other phantom values and vice versa

Organ	Average relative % difference to ICRP			Overall mean % difference	Standard deviation of % difference
	XCAT	Literature	RT-PAL		
Bladder	-27.8	-77.4	11.2	-31.3	44.4
Brain	-0.9	-2.4	12.9	3.2	8.5
Eyes	12.7	-4.6	44.2	17.4	24.7
Gallbladder	-71.8	-32.5	-88.3	-64.2	28.7
Heart	5.6	-64.0	-7.0	-21.8	37.1
Kidneys	16.1	-34.6	-4.7	-7.7	25.5
Large Bowel	17.3	-39.4	28.2	2.0	36.3
Liver	9.4	7.9	5.0	7.4	2.3
Lungs	-4.7	-12.0	-15.6	-10.7	5.6
Oesophagus	-31.2	-38.2	-43.3	-37.5	6.0
Oral Cavity					
Pancreas	-14.9	-2.4	-56.1	-24.5	28.1
Rectum	477.7		1,620.8	1,049.2	808.3
Salivary Glands	12.9	1.0	2.4	5.4	6.5
Small Bowel	-18.7	-47.9	28.4	-12.7	38.5
Spinal Cord	41.1		-8.0	16.6	34.7
Spleen	48.1	67.6	69.5	61.7	11.8
Stomach	-26.1	-62.3	-26.4	-38.3	20.8
Thyroid	33.7	62.1	11.8	35.9	25.2
AVERAGE	**26.6**	**-17.4**	**88.1**	**32.4**	**53.0**

these individuals may not be entirely empty at the time of the scan, in turn affecting the volume, making it greater than the volume of an empty bladder and stomach which is what the Literature may be based on.

Table 4
All the linear regression equations for each phantom and the respective organ. There is no equation for the oral cavity, rectum and spinal cord due to a lack of data

Organ	Linear fit equation			
	ICRP	XCAT	Literature	RT-PAL
Bladder	$y = 11.072x + 12.982$	$y = 7.6329x + 11.304$	$y = 1.9394x + 6.0036$	$y = 12.555x + 13.143$
Brain	$y = 26.044x + 1001.2$	$y = 16.11x + 1065.9$	$y = 25.275x + 978.22$	$y = 14.148x + 1246.7$
Eyes	$y = 0.4029x + 7.6118$	$y = 0.3656x + 9.2193$	$y = 0.3762x + 7.3224$	$y = 0.4847x + 11.675$
Gallbladder	$y = 5.85x + 8.0318$	$y = 0.9169x + 6.2794$	$y = 3.7893x + 6.2766$	$y = 0.3478x + 2.7695$
Heart	$y = 33.544x + 46.019$	$y = 37.157x + 39.185$	$y = 13.008x + 11.465$	$y = 22.56x + 90.172$
Kidneys	$y = 12.789x + 53.263$	$y = 18.365x + 39.789$	$y = 8.5258x + 33.846$	$y = 11.535x + 54.861$
Large Bowel	$y = 26.441x + 63.355$	$y = 31.198x + 73.188$	$y = 17.357x + 30.529$	$y = 27.064x + 121.21$
Liver	$y = 64.423x + 221.19$	$y = 77.397x + 199.61$	$y = 61.835x + 285.7$	$y = 63.153x + 259.54$
Lungs	$y = 149.83x + 52.73$	$y = 129.01x + 117.55$	$y = 126.43x - 73.043$	$y = 100.29x + 171.75$
Oesophagus	$y = 2.2602x + 6.2671$	$y = 2.2559x - 0.1227$	$y = 1.7248x + 1.9242$	$y = 1.0149x + 5.1522$
Oral Cavity		$y = 6.9388x + 33.272$	$y = 2.708x + 71.46$	$y = 3.6987x + 91.598$
Pancreas	$y = 5.9637x + 8.4737$	$y = 5.7764x + 3.344$	$y = 5.8296x + 8.2185$	$y = 2.2654x + 5.6724$
Rectum	$y = 0.2838x + 0.6619$	$y = 2.1372x + 0.916$		$y = 4.6308x + 12.866$
Salivary Glands	$y = 2.8772x + 18.609$	$y = 3.2325x + 21.117$	$y = 2.8825x + 18.959$	$y = 2.4114x + 22.575$
Small Bowel	$y = 73.724x - 30.759$	$y = 43.734x + 104.86$	$y = 30.014x + 57.442$	$y = 52.999x + 244.53$
Spinal Cord	$y = 2.1765x + 21.538$	$y = 3.3873x + 28.216$		$y = 2.3615x + 17.337$
Spleen	$y = 6.1677x + 13.781$	$y = 12.408x + 1.4009$	$y = 8.4371x + 34.145$	$y = 8.4845x + 34.787$
Stomach	$y = 15.954x + 56.319$	$y = 9.003x + 58.745$	$y = 7.2687x + 13.538$	$y = 14.204x + 26.297$
Thyroid	$y = 0.7165x + 0.4275$	$y = 0.9493x - 0.6134$	$y = 0.7187x + 2.929$	$y = 0.3478x + 2.7695$

RT-PAL overall is the least similar to ICRP (highest P.D of 88.1%) – a positive P.D shows that generally RT-PAL values tend to be higher than the ICRP values, although the very large rectum P.D may greatly influence this P.D. All of the RT-PAL linear fits have high R^2 values (except for the brain), i.e. strong fits, with p-values <0.05 so they are statistically significant too. The biggest difference between the two phantoms is that RT-PAL is based on patients undergoing CSI, but ICRP is all healthy patient data. In CSI, radiation is administered to the entire brain and spinal cord to ensure that any cancer cells that may have metastasised to other areas of the central nervous system (CNS) are killed, which means that a very large volume of the body receives radiation [29]. Anatomically, many major organs – including the ones analysed in this review – are found near the brain and spinal cord so these organs will also indirectly receive some of this radiation dose.

The very large P.D for the rectum (1,620.8%) is noteworthy as it shows that the rectal volume in the RT-PAL phantom is a lot greater than the ICRP volume, even though the rectum may not receive the highest dose of stray radiation [30]. The p-values for the RT-PAL and ICRP rectum fits are both <0.05 so they are statistically significant, therefore the P.D calculated is also likely to be true. The function of the rectum is to store faeces until it is egested out of the body – this could potentially explain the large difference in volume as the amounts of faeces stored in the rectums of the RT-PAL patients compared to the ICRP individuals could vary [31]. Perhaps there was an inconsistency across the phantoms in the segmentation of the rectum. Maybe the ICRP contour included the volume of the rectal wall, whereas the other phantoms included the lumen as well as the wall, or poor contrast at organ boundaries in the scans led to the irregularity in organ contour. The same explanations could also be applied to the very high XCAT P.D for the rectum (477.7%), however with the XCAT rectum data, the R^2 value indicates a poor fit and this weak correlation is statistically significant (p-value <0.05) so it could be argued that this P.D is not entirely justifiable. Excluding the rectum P.D, on average RT-PAL is then only 2.1% smaller than ICRP, indicating that the rectum heavily influences the average P.D and the phantom is more similar to ICRP than even the literature data. Hence, it could potentially be used to model a paediatric population.

Splenic volume in the RT-PAL phantom is 69.5% greater than in the ICRP phantom. Splenomegaly i.e. splenic enlargement can occur in paediatric cancers, sometimes, but not always, because of chemotherapy toxicity – the study by El Chediak *et al.*, shows that an increase in splenic volume may be an indicator of oxaliplatin – an alkylating chemotherapeutic agent – toxicity [32,33]. The RT-PAL models are based on historical paediatric cancer patients so it is possible that they have enlarged spleens from previous chemotherapy, which would explain the larger volume compared to ICRP.

The pancreas is a very radiation-sensitive organ and can lose volume and function after receiving an unwanted dose of radiation, as shown in the study by Gemici *et al.* – ideally it should be treated as an organ at risk from radiation toxicity [34]. The study mentioned would therefore explain the pancreas P.D to ICRP observed for RT-PAL which is -56.1%. This indicates that the RT-PAL pancreatic volume is lower than the ICRP and because RT-PAL patients have been given CSI, they may have had unintentional radiation to the

Table 5
The R^2 values and p-values for each regression model for that respective organ. A p-value less than 0.05 indicates a statistically significant correlation and vice versa (95% confidence level). The rectum and spinal cord for literature and oral cavity for ICRP have been left blank due to a lack of data. The key is the small table

Organ	ICRP		XCAT		Literature		RT-PAL	
	R2 value	p-value	R2 value	p-value	R2 value	p-value	R2 value	p-value
Bladder	0.993	<0.05	0.439	<0.05	0.992	<0.05	0.920	<0.05
Brain	0.810	>0.05	0.393	<0.05	0.781	>0.05	0.170	<0.05
Eyes	0.844	>0.05	0.877	<0.05	0.833	>0.05	0.840	<0.05
Gallbladder	0.956	<0.05	0.177	<0.05	0.627	>0.05	0.683	<0.05
Heart	0.988	<0.05	0.792	<0.05	0.765	<0.05	0.969	<0.05
Kidneys	0.997	<0.05	0.747	<0.05	0.985	<0.05	0.898	<0.05
Large Bowel	0.977	<0.05	0.686	<0.05	1.000	<0.05	0.883	<0.05
Liver	0.981	<0.05	0.757	<0.05	0.993	<0.05	0.938	<0.05
Lungs	0.912	<0.05	0.756	<0.05	0.788	<0.05	0.955	<0.05
Oesophagus	0.990	<0.05	0.900	<0.05	0.980	<0.05	0.955	<0.05
Oral Cavity			0.852	<0.05	1.000	<0.05	0.776	<0.05
Pancreas	0.966	<0.05	0.902	<0.05	0.962	<0.05	0.890	<0.05
Rectum	0.981	<0.05	0.437	<0.05			0.950	<0.05
Salivary Glands	0.961	<0.05	0.879	<0.05	0.965	<0.05	0.907	<0.05
Small Bowel	0.963	<0.05	0.710	<0.05	0.999	<0.05	0.892	<0.05
Spinal Cord	0.897	>0.05	0.662	<0.05			0.920	<0.05
Spleen	0.813	>0.05	0.714	<0.05	0.917	<0.05	0.856	<0.05
Stomach	0.972	<0.05	0.264	<0.05	0.996	<0.05	0.905	<0.05
Thyroid	0.983	<0.05	0.905	<0.05	0.977	<0.05	0.683	<0.05
AVERAGE	**0.943**		**0.676**		**0.915**		**0.842**	

R2 value	Interpretation
0–0.2	Very poor fit
0.2–0.5	Poor fit
0.5–0.7	Average fit
0.7–0.9	Good fit
0.9–1	Very good fit
1	Perfect fit
p-value	**Interpretation**
<0.05	Statistically Significant
>0.05	Statistically Insignificant

pancreas as well, which could lead to the decrease in its volume. Another study by Regnell *et al.* shows that pancreatic volume is 27% smaller in type 1 diabetic paediatric patients than in healthy patients [35]. Potentially this means that RT-PAL could be used as a model for the pancreatic volume in type 1 diabetic patients as well because RT-PAL has a smaller pancreatic volume than normal.

The XCAT phantom is almost as similar to the ICRP as literature because its average P.D is 26.6% i.e., on the lower end and excluding the outlier rectal value, this P.D falls to be 0.0% i.e., the two phantoms are virtually the same on average. A potential explanation for the general similarity could be because patient dataset selection for the XCAT models was based on the height and weight values found in ICRP publications, and the organ masses in the XCAT phantoms were matched to the reference values found in Publication 89. This means that the organ volume will be quite similar between the two phantoms and any small differences could either be caused by variations in patient datasets or because XCAT model creation involved the merging of different sources of data – they used cadaver data and scaled-down versions of their adult phantoms as well.

The gallbladder P.Ds for XCAT (-71.8%) and RT-PAL (-88.3%) are fairly high, with both being negative so the ICRP volume is larger than the other two's volumes. This could be because the ICRP phantoms are perhaps more generous with the organ contour, making it a larger volume than it would anatomically be. This seems plausible because the literature P.D is also negative and not small (-32.5%) while the literature data for this organ is partly from Publication 89; so, P.D is expected to be smaller. The other part of the literature data is from a paper looking at gallbladder volume in normal versus appendicitis paediatric patients so average data for both groups have also been used in this review. The paper observed that gallbladder volume is significantly higher in appendicitis patients (p-value=0.004) but even then, in this review's analysis, literature volume seems to be less than the ICRP volume [16]. On the other hand, it could be argued that the gallbladder is very small, about 7–10 cm by 3–4 cm in adults, so in children it

would be even smaller, potentially making it a very difficult organ to segment, hence leading to the underestimation of organ volume for the XCAT and RT-PAL phantoms [36]. Either way however, more research needs to be conducted before a conclusion is made regarding the contour.

Age

As age increases, the similarity to ICRP also increases across the phantoms, as seen by the decreasing average P.D in Table 2 so the models are overall more accurate for older children than younger children. There is also less variation in the P.Ds for each age as age increases, as reflected by the decreasing S.D. Scientifically, growth velocity is the highest around birth and this decreases as the child gets older – this could explain the large P.D to ICRP and substantial variation at age 1 [37]. Another reason could be that when creating the models, it might be harder to accurately segment each organ because of the smaller relative organ size, leading to inconsistencies in the organ contours across the phantoms, hence generating large P.Ds relative to ICRP and large S.Ds for 1-year-olds. But children have a second growth spurt during adolescence, in which growth velocity again accelerates, and there is variation in growth rates between children as well, which will then influence their organ volume and will perhaps lead to more variation in P.Ds to ICRP in older children [37]. However, the results of this study do not necessarily reflect this as S.D decreases with age when scientifically it would be expected to increase or remain constant.

The number of negative P.Ds also increases with age. In 15-year-old, for majority of the organs the ICRP volume is larger than the other phantom value and vice versa for 1 year-old. This could be due to the age brackets used for XCAT and RT-PAL. For example, for both the 1-year-old value bracket includes ages a few years older than 1 so the organ volumes for these phantoms will naturally be bigger than the ICRP 1 year-old phantom, hence resulting in mostly positive P.Ds. The bracket for the RT-PAL 15-year-old value includes ages a few years less than 15 so the volumes are naturally smaller than the ICRP, which could then cause the negative P.Ds. However, the XCAT age bracket includes ages older than 15 so this should counteract the effects of the smaller RT-PAL value on the average P.D but this does not seem to be the case.

The rectal volume for all other phantoms is always more than 1,000 times greater than ICRP with the highest variation in its data, as displayed by the high P.D and S.D across the ages. Reasons for this disparity in volume have previously been discussed and can still be applied in this context. Larger, more major organs such as the brain, heart and lungs have P.Ds that are towards the lower end of the spectrum, i.e. they are modelled better in general for all ages, perhaps because they are easier to segment, as opposed to smaller organs like the gallbladder, spleen and thyroid. It could be argued that it is more important for the major organs to be modelled more accurately as radiation damage to them could severely impact regular bodily functions. For example, the heart – radiation toxicity can lead to advanced/precocious coronary heart disease, and this is more likely in paediatric patients receiving radiation [38]. The lungs – inflammation of lung tissue and radiation fibrosis can occur which can impact pulmonary function, preventing oxygen from being absorbed efficiently [39]. But damage to a smaller organ such as the thyroid may have less of an impact. Primary hypothyroidism due to radiation damage can arise in 20–30% of patients who receive radiation in the neck region, but this can be treated fairly easily via a daily oral dose of levothyroxine to restore thyroid hormone levels [40,41].

Another observation can be made by using Table 4. The x coefficients of these equations indicate the rate of increase/decrease in organ volume (y) as age (x) increases. The y-intercept indicates the perceived organ volume at 0 years (newborn). All of the equations have positive x coefficients i.e. organ volume increases as age increases. The larger the x coefficient, the faster the growth rate – organs like the liver, lungs and small bowel have the largest x coefficients so they tend to grow the fastest. The brain in children is large and fast growing, especially in the early years of life and this is reflected by the relatively large x coefficients and the largest y intercepts, consistently across all phantoms [42]. In Table 2, some organs including the heart, lungs and small bowel, start with positive P.Ds to ICRP but as age increases, the P.D becomes increasingly negative. This could be explained by the x coefficients of the regression equations. For the small bowel, the ICRP coefficient is 1.7, 2.5 and 1.4 times greater than XCAT, literature and RT-PAL coefficients respectively, meaning that the ICRP small bowel volume increases faster than the other three, even though the ICRP is initially smaller than the other phantoms. ICRP volume will increase faster with age, eventually making it greater than the other phantoms' volume, resulting in the described change in P.D. The same reasoning could be applied for the heart and lung trend in P.D. However, for the heart, the XCAT coefficient is 1.1 times bigger than the ICRP coefficient, but perhaps this is not large enough to have a substantial impact on P.D.

Limitations

This review does have its limitations, mainly within the literature data. Because of a lack of papers for certain organs, Publication 89 had to be used which is not an entirely fair comparison since it should generally be very similar to the ICRP volumes. The absence of ICRP data for the oral cavity was another hindrance as it meant that it could not be analysed at all because all the comparisons were made relative to ICRP. Not many studies were found for patients with different diseases either – majority of the papers were for healthy patients so there were not that many findings on whether other organ-specific diseases can affect organ volume. Due to time constraints, not all of the intended statistical tests could be carried out and if given more time these would be executed, making this study even more informative. No statistical test to get a p-value was done for the age results, like the organ results, to see if the P.Ds obtained are worth noting. Perhaps doing a statistical test for the comparison of the linear fit slopes would have been

more efficient rather than comparing them using a combination of the P.D, R^2 and p-values.

Conclusion

The main application for these phantoms is to understand and mitigate radiation-induced side effects. Although in clinical practice, the assumption that a particular age-appropriate model can be applied to all children in that age category may not be the right approach as children grow at different rates to each other. Some children have their growth spurts earlier and some have them much later, therefore it may be inappropriate to assume that an age phantom can fit all children at that age. Perhaps a phantom should be chosen to model a child depending on their height and weight, for example, rather than their age. Nevertheless, the models can be used to model a paediatric population but may need to be improved to make them more accurate for certain organs. The XCAT and RT-PAL models may need to be refined for certain organs such as the gallbladder, rectum and spleen, especially for the younger ages, possibly by basing them on literature data/data from multiple sources to then make them more accurate and similar to ICRP. Seeing as though the XCAT model is overall quite similar to ICRP, these two phantoms could be used to model healthy patients prior to radiotherapy to prevent second cancers/other effects. The two could be used in combination – XCAT for a particular organ and ICRP for another, but more research needs to be done to see which one of the two is a better model for each organ. Because RT-PAL shows potential changes in organ size whilst undergoing radiotherapy to a large volume of the body, this phantom could be used for cancer patients who have already had or are going through a round of radiotherapy, to prevent any further toxicities to organs that receive unwanted radiation.

Author contribution

VA: Conceptualization, Investigation, Writing—original draft, Writing—review & editing. AG: Investigation, Writing—review & editing. CAL: Validation, Writing—review & editing. SA: Validation, Writing—review & editing. VP: Validation, Writing—review & editing. ER: Writing—review & editing, Supervision. SB: Writing—review & editing, Supervision. All authors read and approved the submitted version.

Conflict of Interest

The authors declare no conflict of interest.

Appendix A. Supplementary data

Supplementary data to this article can be found online at https://doi.org/10.1016/j.clon.2024.06.051.

References

[1] Vermund H, Gollin FF. Mechanisms of action of radiotherapy and chemotherapeutic adjuvants. A review. *Cancer* 1968; 21(1):58–76. https://doi.org/10.1002/1097-0142:(196801)21:1<58::AID-CNCR2820210110>3.0.CO;2-5.

[2] Barazzuol L, Coppes RP, van Luijk P. Prevention and treatment of radiotherapy-induced side effects. *Mol Oncol* 2020;14(7): 1538–1554. https://doi.org/10.1002/1878-0261.12750.

[3] DeNunzio NJ, Yock TI. Modern Radiotherapy for Pediatric Brain Tumors. *Cancers (Basel)* 2020;12(6):1533. https://doi.org/10.3390/cancers12061533.

[4] Varchena V. Pediatric phantoms. *Pediatr Radiol* 2002;32(4): 280–284. https://doi.org/10.1007/s00247-002-0681-z.

[5] Lee TF, Huang EY. The different dose-volume effects of normal tissue complication probability using LASSO for acute small-bowel toxicity during radiotherapy in gynecological patients with or without prior abdominal surgery. *BioMed Res Int* 2014; 2014(1):e143020. https://doi.org/10.1155/2014/143020.

[6] Bolch WE, Eckerman K, Endo A, Hunt JGS, Jokisch DW, Kim CH, *et al.* ICRP Publication 143: Paediatric Reference Computational Phantoms. *Ann ICRP* 2020;49(1):5–297. https://doi.org/10.1177/0146645320915031.

[7] ICRP. Adult Reference Computational Phantoms. ICRP Publication 110. *Ann ICRP* 2009;39:3–5.

[8] Norris H, Zhang Y, Bond J, Sturgeon GM, Minhas A, Tward DJ, *et al.* A set of 4D pediatric XCAT reference phantoms for multimodality research. *Med Phys* 2014;41(3):033701. https://doi.org/10.1118/1.4864238.

[9] Segars WP, Norris H, Sturgeon GM, Zhang Y, Bond J, Minhas A, *et al.* The development of a population of 4D pediatric XCAT phantoms for imaging research and optimization. *Med Phys* 2015;42(8):4719–4726. https://doi.org/10.1118/1.4926847.

[10] Veiga C, Lim P, Anaya VM, Chandy E, Ahmad R, D'Souza D, *et al.* Atlas construction and spatial normalisation to facilitate radiation-induced late effects research in childhood cancer. *Phys Med Biol* 2021;66(10):105005. https://doi.org/10.1088/1361-6560/abf010.

[11] Malek S, Mosleh M, Dhillon SK, Milow P. Bioimage Informatics. In: Ranganathan S, Gribskov M, Nakai K, Schönbach C, editors. *Encyclopedia of bioinformatics and computational biology*. Oxford: Academic Press; 2019. p. 993–1010.

[12] Veiga C. Welcome to the Radiotherapy Paediatric Atlas (RT-PAL) Project Page. [cited 2022 April 11]. Available from: https://cmic-rt.github.io/RT-PAL/.

[13] Basic anatomical and physiological data for use in radiological protection: reference values. A report of age- and gender-related differences in the anatomical and physiological characteristics of reference individuals. ICRP Publication 89. *Ann ICRP* 2002;32(3–4):5–265.

[14] [cited 2022 Apr 3]. Available from:*Report of the task group on reference man ICRP Publication 23* 1975 https://journals.sagepub.com/doi/abs/10.1016/0146-6453%2880%2990047-0.

[15] Dekaban AS. Changes in brain weights during the span of human life: relation of brain weights to body heights and body weights. *Ann Neurol* 1978;4(4):345–356. https://doi.org/10.1002/ana.410040410.

[16] Yalcin A, Demir B, Demir M, Firinci B, Polat G, Pirimoglu B, *et al.* Association of Gallbladder Volume and Wall Thickness With Acute Appendicitis in Pediatric Patients. *Pediatr Emerg Care* 2022;38(2):e443–e446. https://doi.org/10.1097/PEC.0000000000002625.

[17] Coppoletta JM, Wolbach SB. Body Length and Organ Weights of Infants and Children: A Study of the Body Length and

Normal Weights of the More Important Vital Organs of the Body between Birth and Twelve Years of Age. *Am J Pathol* 1933;9(1):55–70.
[18] Molina DK, DiMaio VJ. Normal Organ Weights in Women: Part I-The Heart. *Am J Forensic Med Pathol* 2015;36(3):176–181. https://doi.org/10.1097/PAF.0000000000000174.
[19] Molina DK, DiMaio VJ. Normal organ weights in men: part I-the heart. *Am J Forensic Med Pathol* 2012;33(4):362–367. https://doi.org/10.1097/PAF.0b013e31823d298b.
[20] Kim DW, Ahn HG, Kim J, Yoon CS, Kim JH, Yang S. Advanced Kidney Volume Measurement Method Using Ultrasonography with Artificial Intelligence-Based Hybrid Learning in Children. *Sensors (Basel)* 2021;21(20):6846. https://doi.org/10.3390/s21206846.
[21] Herden U, Wischhusen F, Heinemann A, Ganschow R, Grabhorn E, Vettorazzi E, *et al*. A formula to calculate the standard liver volume in children and its application in pediatric liver transplantation. *Transpl Int* 2013;26(12):1217–1224. https://doi.org/10.1111/tri.12198.
[22] Molina DK, DiMaio VJ. Normal Organ Weights in Women: Part II-The Brain, Lungs, Liver, Spleen, and Kidneys. *Am J Forensic Med Pathol* 2015;36(3):182–187. https://doi.org/10.1097/PAF.0000000000000175.
[23] Molina DK, DiMaio VJ. Normal organ weights in men: part II-the brain, lungs, liver, spleen, and kidneys. *Am J Forensic Med Pathol* 2012;33(4):368–372. https://doi.org/10.1097/PAF.0b013e31823d29ad.
[24] Ding X, Suzuki S, Shiga M, Ohbayashi N, Kurabayashi T, Moriyama K. Evaluation of tongue volume and oral cavity capacity using cone-beam computed tomography. *Odontology* 2018;106(3):266–273. https://doi.org/10.1007/s10266-017-0335-0.
[25] de la Grandmaison GL, Clairand I, Durigon M. Organ weight in 684 adult autopsies: new tables for a Caucasoid population. *Forensic Sci Int* 2001;119(2):149–154. https://doi.org/10.1016/S0379-0738(00)00401-1.
[26] Nemati M, Hajalioghli P, Jahed S, Behzadmehr R, Rafeey M, Fouladi DF. Normal Values of Spleen Length and Volume: An Ultrasonographic Study in Children. *Ultrasound Med Biol* 2016;42(8):1771–1778. https://doi.org/10.1016/j.ultrasmedbio.2016.03.005.
[27] Scammon RE. Some graphs and tables illustrating the growth of the human stomach. *Am J Dis Child* 1919;17:395–422. https://doi.org/10.1001/archpedi.1919.04110300020002.
[28] Hegedüs L, Perrild H, Poulsen LR, Andersen JR, Holm B, Schnohr P, *et al*. The determination of thyroid volume by ultrasound and its relationship to body weight, age, and sex in normal subjects. *J Clin Endocrinol Metab* 1983;56(2):260–263. https://doi.org/10.1210/jcem-56-2-260.
[29] Royal Marsden Patient Information Library. [cited 2022 Apr 19]. Craniospinal radiotherapy. Available from: https://patientinfolibrary.royalmarsden.nhs.uk/craniospinal-radiotherapy.
[30] Taddei PJ, Mirkovic D, Fontenot JD, Giebeler A, Zheng Y, Kornguth D, *et al*. Stray radiation dose and second cancer risk for a pediatric patient receiving craniospinal irradiation with proton beams. *Phys Med Biol* 2009;54(8):2259–2275. https://doi.org/10.1088/0031-9155/54/8/001.
[31] Cleveland Clinic. Digestive System. [cited 2022 Apr 19]. Available from: https://my.clevelandclinic.org/health/body/7041-digestive-system.
[32] O'Reilly RA. Splenomegaly in 2,505 patients in a large university medical center from 1913 to 1995. 1913 to 1962: 2,056 patients. *West J Med* 1998;169(2):78–87.
[33] El Chediak A, Haydar AA, Hakim A, Massih SA, Hilal L, Mukherji D, *et al*. Increase in spleen volume as a predictor of oxaliplatin toxicity. *Ther Clin Risk Manag* 2018;14:653–657. https://doi.org/10.2147/TCRM.S150968.
[34] Gemici C, Yaprak G, Ozdemir S, Baysal T, Seseogullari OO, Ozyurt H. Volumetric decrease of pancreas after abdominal irradiation, it is time to consider pancreas as an organ at risk for radiotherapy planning. *Radiat Oncol* 2018;13(1):238. https://doi.org/10.1186/s13014-018-1189-5.
[35] Regnell SE, Peterson P, Trinh L, Broberg P, Leander P, Lernmark Å, *et al*. Pancreas volume and fat fraction in children with Type 1 diabetes. *Diabet Med* 2016;33(10):1374–1379. https://doi.org/10.1111/dme.13115.
[36] Sriselvakumar S. Radiopaedia. Gallbladder. Radiopaedia.org. [cited 2023 Dec 28]. Available from: https://radiopaedia.org/articles/gallbladder?lang=gb.
[37] Tanner JM. Normal growth and techniques of growth assessment. *Clin Endocrinol Metab* 1986;15(3):411–451. https://doi.org/10.1016/S0300-595X(86)80005-6.
[38] Stewart JR, Fajardo LF, Gillette SM, Constine LS. Radiation injury to the heart. *Int J Radiat Oncol Biol Phys* 1995;31(5):1205–1211. https://doi.org/10.1016/0360-3016(94)00656-6.
[39] Gross NJ. The pathogenesis of radiation-induced lung damage. *Lung* 1981;159(3):115–125. https://doi.org/10.1007/BF02713907.
[40] Jereczek-Fossa BA, Alterio D, Jassem J, Gibelli B, Tradati N, Orecchia R. Radiotherapy-induced thyroid disorders. *Cancer Treat Rev* 2004;30(4):369–384. https://doi.org/10.1016/j.ctrv.2003.12.003.
[41] Chakera AJ, Pearce SH, Vaidya B. Treatment for primary hypothyroidism: current approaches and future possibilities. *Drug Des Devel Ther* 2012;6:1–11. https://doi.org/10.2147/DDDT.S12894.
[42] Bogin B. Chapter 11 - The Evolution of Human Growth. In: Cameron N, Bogin B, editors. *Human growth and development*, Second Edition. Boston: Academic Press; 2012. p. 287–324.